Degenerate four-wave mixing with broad-bandwidth pulsed lasers

D. R. Meacher, A. Charlton,* and P. Ewart
Clarendon Laboratory, Parks Road, Oxford, OX1 3PU, United Kingdom

J. Cooper
Joint Institute for Laboratory Astrophysics and National Institute of Standards and Technology, Boulder, Colorado 80309

G. Alber
Faculty of Physics, Albert Ludwigs University, Hermann Herder Strasse 3D, 7800 Freiburg, Federal Republic of Germany
(Received 20 February 1990)

The steady-state theory of degenerate four-wave mixing (DFWM) with broad-bandwidth lasers is extended to treat the time dependence of the interaction allowing calculation of the intensity dependence and saturation behavior of DFWM with pulsed lasers. An experimental study of this intensity dependence as a function of laser bandwidth is reported, showing qualitative agreement with the theory. The line shape of DFWM induced by broad-bandwidth pump fields, probed by a monochromatic probe, is shown to have a Doppler-broadened profile in agreement with the theoretical predictions.

I. INTRODUCTION

Much interest has been shown recently in the effects of the laser bandwidth in atom-field interactions. Effects attributable to the field fluctuations associated with broad-bandwidth radiation have been studied theoretically and experimentally in processes such as laser-induced resonance fluorescence, multiphoton absorption and ionization, and optical double resonance.[1] Such fluctuation effects are also important in optical coherent transient processes that use broadband radiation to achieve high temporal resolution by relying on the short coherence time of the light.[2] Nonlinear parametric processes will also be strongly affected by the stochastic processes of broadband laser fields. The influence of these fluctuations has been shown to be very important in a number of practical schemes such as coherent anti-Stokes Raman scattering (CARS). The noise properties of the laser field play a limiting role in the precision of measurement based on CARS spectra.[3] Another parametric process of practical importance is resonant degenerate four-wave mixing (DFWM), which has been extensively reviewed.[4] In a recent paper we presented a revised theory of resonant DFWM with broad-bandwidth lasers.[5] This theory treated the steady-state situation and allowed calculation of the saturation behavior of the signal as a function of the bandwidth of both pump and probe beams.

Steady-state conditions are usually encountered in experiments with cw lasers where the radiation is effectively monochromatic and the conventional coherent radiation theory of DFWM of Abrams and Lind[6] may be applied. It should be noted, however, that significant effects arising from the finite width of even single-mode lasers have been observed in processes such as resonance fluorescence and two-photon absorption. These processes have been studied theoretically using a phase-diffusion model and experimentally verified using a specially tailored laser line shape to reproduce a phase-diffusing field.[7] Transient behavior of the relaxation to the steady state in two-photon resonant four-wave mixing with broad-bandwidth pump fields has been considered theoretically.[8]

In many situations pulsed lasers are employed for DFWM where the pulse duration is too short to allow steady-state conditions to be established. In this case a time-dependent theory is needed. Furthermore, the fluctuations of amplitude and phase associated with the finite spectral width of pulsed lasers are more characteristic of a chaotic field than a phase-diffusing type. In the present work we present an extension of our previous theory[5] to give a time-dependent description of DFWM more appropriate to the modeling of experiments using pulsed, high power lasers. We report also, results of an experimental study of resonant DFWM in Na vapor using a variable bandwidth pulsed laser giving an approximately chaotic-type field.

In Sec. II we present the basic theoretical description of four-wave mixing (FWM) with broad-bandwidth fields. We show how the required averaging over the stochastic processes involved may be carried out while retaining the explicit time dependence of the coupled density-matrix equations. In Sec. III we describe experiments that measure first the dependence of the DFWM signal on the intensity of the pump beams for different laser bandwidths, and second, the spectral line shape of the signal using a monochromatic probe. Finally, in Sec. IV, we discuss the experimental results in relation to the theory.

II. THEORY

Our treatment is based on our steady-state theory of DFWM presented previously, where the procedures are given in detail.[5] As before we restrict ourselves to the situation of an optically thin medium, composed of two-level atoms subjected to two intense, counterpropagating pump beams and a weak probe beam. The field description is given in Ref. 5 and represents a chaotic field with a

Lorentzian shaped spectrum of width [half width at half maximum (HWHM)] b, which exceeds all other relaxation rates in the problem. The spectral width of the weak probe p is in general different from b, and may be set equal to zero to represent a monochromatic field. The interaction of the fields with the atoms is described by the Rabi frequencies $\Omega(\mathbf{x},t)$ and $\Omega_3(\mathbf{x},t)$ for pump and probe, respectively.

A. Basic equations

We consider the laser fields to interact with an atom having ground and excited energy levels E_g and E_e, respectively, such that the laser frequencies ω_i are near resonance. The strong pump fields and a weak probe field have frequencies ω_1 and ω_3, respectively. The evolution of the atomic response is described using the density matrix ρ by the Liouville equation

$$i\hbar\frac{d\rho}{dt}=[\hat{H},\rho]+\mathcal{D} , \tag{1}$$

where

$$\hat{H}=\hat{H}_0+\hbar[\Omega(\mathbf{x},t)e^{-i\omega_1 t}+\Omega_3(\mathbf{x},t)e^{-i(\omega_3 t-k_3 x)}+\text{c.c.}] ,$$

$\hat{H}_0$ is the unperturbed atomic Hamiltonian, and $\mathcal{D}$ represents damping terms. The damping terms are dependent on the longitudinal and transverse relaxation rates of the atom, κ and Γ, respectively.

Expanding the density matrix in orders m and n of the pump and probe fields, respectively,

$$\rho=\sum_{m,n}\rho^{mn}e^{-i[m\omega_1 t+n(\omega_3 t-k_3 x)]} ,$$

we obtain the following set of equations:

$$\left[\frac{d}{dt}+\kappa\right]\rho_0(\mathbf{x},t)=\kappa-2\,\mathrm{Im}[\Omega^*(\mathbf{x},t)\rho_1(\mathbf{x},t)] , \tag{2a}$$

$$\left[\frac{d}{dt}-i\Delta+\Gamma\right]\rho_1(\mathbf{x},t)=(i/2)\Omega(\mathbf{x},t)\rho_0(\mathbf{x},t)+(i/2)\Omega_3\rho_4(\mathbf{x},t) , \tag{2b}$$

$$\left[\frac{d}{dt}+i\Delta_2+\Gamma\right]\rho_3(\mathbf{x},t=(-i/2)\Omega_3^*\rho_0(\mathbf{x},t)-(i/2)\Omega^*(\mathbf{x},t)\rho_4(\mathbf{x},t) , \tag{2c}$$

$$\left[\frac{d}{dt}-i\delta+\kappa\right]\rho_4(\mathbf{x},t)=i\Omega^*(\mathbf{x},t)\rho_5(\mathbf{x},t)-i\Omega(\mathbf{x},t)\rho_3(\mathbf{x},t)+i\Omega_3^*\rho_1(\mathbf{x},t) , \tag{2d}$$

$$\left[\frac{d}{dt}-i\Delta_3+\Gamma\right]\rho_5(\mathbf{x},t)=(i/2)\Omega(\mathbf{x},t)\rho_4(\mathbf{x},t) , \tag{2e}$$

where we have written

$$\rho_0(\mathbf{x},t)=\rho_{g\text{-}g}^{00}(\mathbf{x},t)-\rho_{e\text{-}e}^{00}(\mathbf{x},t),\quad \rho_1(\mathbf{x},t)=\rho_{e\text{-}g}^{10}(\mathbf{x},t) ,$$

$$\rho_2(\mathbf{x},t)=[\rho_1(\mathbf{x},t)]^*,\quad \rho_3(\mathbf{x},t)=\rho_{g\text{-}e}^{0-1}(\mathbf{x},t) ,$$

$$\rho_4(\mathbf{x},t)=\rho_{g\text{-}g}^{1,-1}(\mathbf{x},t)-\rho_{e\text{-}e}^{1,-1}(\mathbf{x},t),\quad \rho_5(\mathbf{x},t)=\rho_{e\text{-}g}^{2,-1}(\mathbf{x},t) ,$$

Δ is the detuning of the pump waves given by

$$\Delta=(E_g-E_e-\hbar\omega_1)/\hbar ,$$

and those of the probe Δ_2 and generated fourth wave Δ_3 are

$$\Delta_2=(E_e-E_g-\hbar\omega_3)/\hbar ,$$

$$\Delta_3=(E_g-E_e+2\hbar\omega_1-\hbar\omega_3)/\hbar .$$

δ is the pump-probe detuning given by

$$\delta=\omega_1-\omega_3 .$$

The observed signal arises from a polarization described, in general, by a product of density-matrix elements. Now, defining these products by $A_{ij}(\mathbf{x},\mathbf{x}',t)=\rho_i(\mathbf{x},t)[\rho_j(\mathbf{x}',t)]^*$, for $i,j=1,\ldots,5$, we derive differential equations for their evolution from which we can find the stochastic averages of the products of the A_{ij} and the field variables. The polarization responsible for the radiated signal beam is given by the term $A_{55}(\mathbf{x},\mathbf{x}',t)$. The generated signal is then found, in the slowly varying envelope approximation, by integrating this averaged polarization over the interaction length l:

$$\langle I_4\rangle=\frac{(2\omega_1-\omega_3)^2n^2|\mu_{e\text{-}g}|^2}{2\epsilon_0 c}\times\int_0^l\int_0^l dx\,dx'\langle A_{55}(\mathbf{x},\mathbf{x}',t)\rangle , \tag{3}$$

where the angular brackets indicate an average over the field fluctuations, $\mu_{e\text{-}g}$ is the atomic dipole moment, and n is the atomic number density. The method of performing the stochastic averaging is described in detail in Ref. 5 in the steady-state limit. In retaining the time dependence we take as our starting point the set of integral equations for the averages over the temporal field fluctuations of the relevant products of density matrix elements and field variables of Ref. 5. For example,

$$\Omega(\mathbf{x})A_{45}(\mathbf{x},\mathbf{x}',t)=i\int_{-\infty}^{t}e^{-(d+a^*)(t-t')}[\{\Omega(\mathbf{x},t)\Omega^*(\mathbf{x},t')\}\{A_{55}(\mathbf{x},\mathbf{x}',t')\}$$
$$+\langle\Omega(\mathbf{x},t)\Omega(\mathbf{x},t')\rangle\langle A_{35}(\mathbf{x},\mathbf{x}',t')\rangle+\Omega_3^*\langle\Omega(\mathbf{x},t)A_{15}(\mathbf{x},\mathbf{x}',t')\rangle$$
$$-\tfrac{1}{2}\langle\Omega(\mathbf{x},t)\Omega^*(\mathbf{x}',t')\rangle\langle A_{44}\Omega(\mathbf{x},\mathbf{x}',t')\rangle]dt' \quad (4)$$

where

$$a=\Gamma-i\Delta_3\ ,$$
$$d=\kappa-i\delta\ .$$

However, we need to consider the general case of fluctuating laser fields, where $\{|\Omega(t)|^2\}$ and $\{|\Omega(t')|^2\}$ may be different. In this case, following Georges,[9] we write for the correlation functions

$$\langle\Omega(\mathbf{x},t)\Omega^*(\mathbf{x},t')\rangle$$
$$=2\langle|\Omega(t)|^2\rangle^{1/2}\langle|\Omega(t')|^2\rangle^{1/2}\exp[-b(t-t')]\ ,$$
$$\langle\Omega(\mathbf{x},t)\Omega(\mathbf{x}',t')\rangle$$
$$=2\langle|\Omega(t)|^2\rangle^{1/2}\langle|\Omega(t')|^2\rangle^{1/2}$$
$$\times\cos[\mathbf{k}\cdot(\mathbf{x}-\mathbf{x}')]\exp[-b(t-t')]\ ,$$

where b is the pump-field bandwidth. For atom-field products involving different times we again use Georges's result[9]

$$\langle\Omega(\mathbf{x},t)A_{15}(\mathbf{x},\mathbf{x}',t')\rangle=\langle\Omega(\mathbf{x},t')A_{15}(\mathbf{x},\mathbf{x}',t')\rangle$$
$$\times\exp[-b(t-t')]\ ,$$

and upon differentiating (4) obtain

$$\left[\frac{d}{dt}+(b+d+a^*)+\eta(t)\right]\langle\Omega(\mathbf{x})A_{45}(\mathbf{x},\mathbf{x}',t)\rangle$$
$$=i[2|\Omega(t)|^2\langle A_{55}(\mathbf{x},\mathbf{x}',t)\rangle+\Omega_3^*\langle\Omega(\mathbf{x})A_{15}(\mathbf{x},\mathbf{x}',t)\rangle$$
$$-|\Omega(t)|^2\langle A_{44}(\mathbf{x},\mathbf{x}',t)\rangle]\ , \quad (5)$$

with

$$\eta(t)\equiv\langle|\Omega(t)|^2\rangle^{-1/2}\frac{d}{dt}\langle|\Omega(t)|^2\rangle^{1/2}\ .$$

In this way we can construct a set of coupled differential equations for $\langle A_{55}(\mathbf{x},\mathbf{x}',t)\rangle$, which determines the *instantaneous* magnitude of the reflected intensity. Since all the correlated terms are now expressed as functions of the same value of time t, we may carry out a *simultaneous* decorrelation of products of atom and field variables. The first few equations are

$$\left[\frac{d}{dt}+2\Gamma\right]\langle A_{55}(\mathbf{x},\mathbf{x}',t)\rangle=-\mathrm{Im}[\langle\Omega(\mathbf{x})A_{45}(\mathbf{x},\mathbf{x}',t)\rangle]\ , \quad (6a)$$

$$\left[\frac{d}{dt}+(b+a^*+d)+\eta(t)\right]\langle\Omega(\mathbf{x})A_{45}(\mathbf{x},\mathbf{x}',t)\rangle$$
$$=i\{2|\Omega(t)|^2\langle A_{55}(\mathbf{x},\mathbf{x}',t)\rangle+\langle\Omega_3^*\langle\Omega(\mathbf{x})A_{15}(\mathbf{x},\mathbf{x}',t)\rangle\rangle$$
$$-|\Omega(t)|^2\langle A_{44}(\mathbf{x},\mathbf{x}',t)\rangle\cos[\mathbf{k}\cdot(\mathbf{x}-\mathbf{x}')]\}\ , \quad (6b)$$

$$\left[\frac{d}{dt}+2\kappa\right]\langle A_{44}(\mathbf{x},\mathbf{x}',t)\rangle$$
$$=-2\,\mathrm{Im}[\langle\Omega^*(\mathbf{x})A_{54}(\mathbf{x},\mathbf{x}',t)\rangle-\langle\Omega(\mathbf{x})A_{34}(\mathbf{x},\mathbf{x}',t)\rangle$$
$$-\langle\Omega_3\langle A_{41}(\mathbf{x},\mathbf{x}',t)\rangle\rangle]\ , \quad (6c)$$

etc.

The full system of decorrelated equations may be solved numerically for arbitrary laser pulse shapes. The solution is valid so long as $\eta\ll b$, i.e., the field envelopes are slowly varying on the time scale of the bandwidth determined fluctuations $1/b$; although they may vary appreciably over the period of an atomic lifetime $1/\kappa$. The final result is found by integrating the calculated atomic response over the interaction length according to Eq. (3). It is more difficult, in the time-dependent situation, to account for atomic motion than in the steady-state case, in which the atomic response was integrated over the Doppler line shape as explained in Ref. 5. The present result does not include the effects of atomic motion which, in the steady-state case, were found to be significant only for intensity levels well above saturation. In the present case of a pulsed interaction such effects are expected to be even less important.

B. Theoretical results

The theory outlined above provides us with two main results. First, we may calculate the exact temporal shape of the DFWM signal for arbitrary input pulse shapes of broad spectral width. Second, we may calculate the intensity dependence and saturation behavior as a function of laser bandwidth for DFWM with pulsed lasers.

Experiments to measure the temporal evolution of the DFWM signal and the bandwidth-dependent pulse shapes are reported elsewhere.[10] For the present we concentrate on the effects of the temporal response on experiments designed to measure the intensity dependence of DFWM as a function of laser bandwidth.

We illustrate the effects by calculating the signal's behavior in time assuming the input lasers have a Gaussian envelope of duration τ_p. In the limit $\tau_p\to\infty$ it can be

readily shown that the signals approach the steady-state values calculated previously.[5] For $\tau_p = 1/\kappa$, i.e., one atomic lifetime, the signal pulse shapes have been calculated for peak intensities equal to 0.2, 1.0, and 5.0 times the bandwidth-dependent saturation level given by $|\Omega_{sat}|^2 = b\kappa$. The results are shown in Fig. 1, and in Fig. 2 we show the results of a similar calculation for a longer pulse $\tau_p = 10/\kappa$. In both cases the bandwidth $b = 100\kappa$. The feature of interest here is not the bandwidth dependence, but the pulse reshaping of the signal that occurs as the pump intensity increases.

The main features of the response are that at low pump intensity $|\Omega|^2 \ll b\kappa$ the signal pulse shape follows that of the incident waves, although it may be narrowed by the nonlinear nature of the interaction. The peak response is delayed with respect to the incident fields approximately by an atomic longitudinal relaxation time. At higher intensities, saturation effects severely alter the temporal behavior of the response. As the laser intensity is increased, the evolution of the signal on the leading edge of the laser pulse is more rapid and the peak reflectivity is reached earlier in time. For sufficiently high intensities the signal then decays rapidly as the atomic transition is saturated

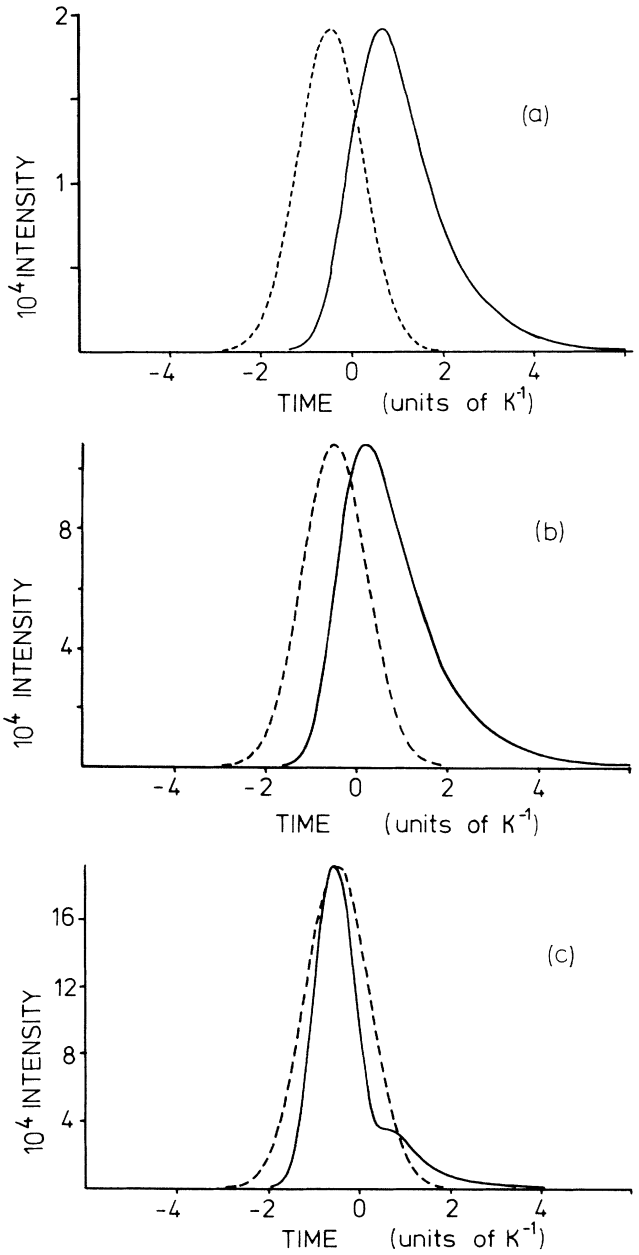

FIG. 1. Calculated DFWM signal pulse shapes for an input laser pulse having a Gaussian envelope of width (HWHM) $\tau_p = 1/\kappa$. Dashed line shows the input pulse; solid lines show the calculated signal pulses for the following intensities: (a) $0.2I_s$, (b) I_s, (c) $5I_s$. Input and signal pulse heights are normalized to the same peak value for comparison of the shape and width.

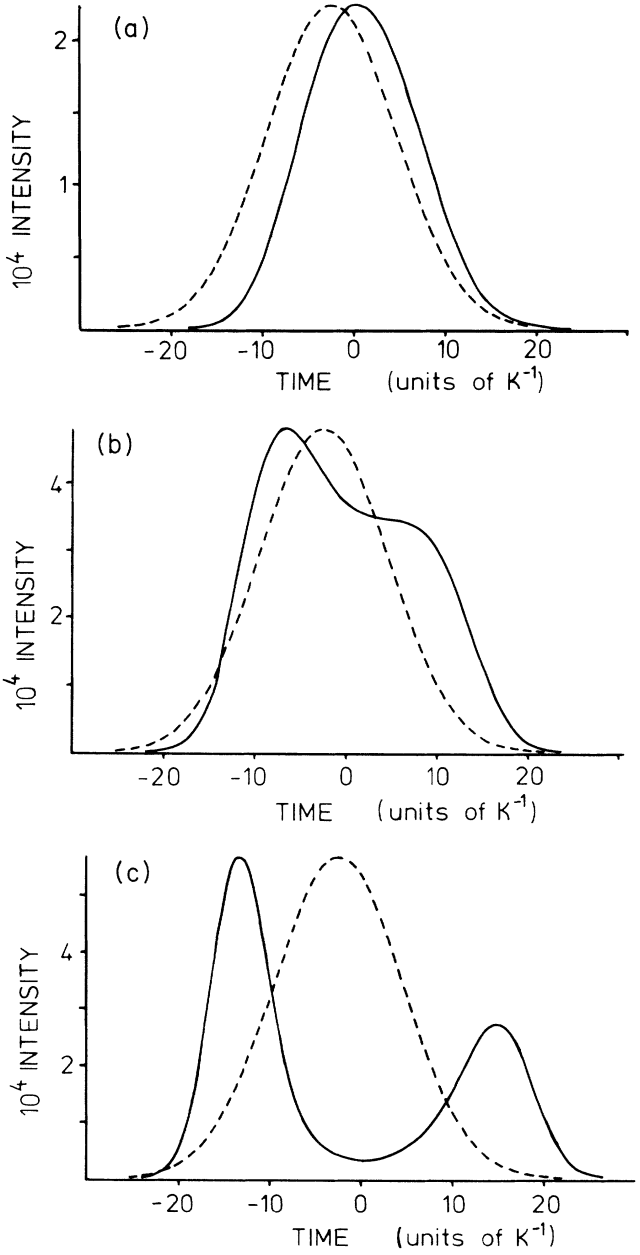

FIG. 2. Calculated DFWM signal pulse shapes (solid lines) as in Fig. 1 but for an input pulse of duration (HWHM) $\tau_p = 10/\kappa$ (dashed lines).

before the end of the laser pulse. Qualitatively similar behavior was predicted for two-photon resonant DFWM in response to a step-function, broad-bandwidth pump field.[8] In the case of the long pump pulse, atomic relaxation allows the signal to recover on the trailing edge of the laser pulse where its intensity is reduced.

In experiments where the signal is detected or averaged only during a finite gate time, e.g., by a boxcar averager, then it is clear from these considerations that the aperture of the gate, and its timing with respect to the incident pulse, will affect the recorded signal level. The measured dependence of the signal on pump intensity I will thus be modified for pulsed interactions. This is illustrated by considering the case of a short laser pulse, such as that of Fig. 1, and a detector whose aperture or gate, of width say $1/2\kappa$, is set to coincide with the peak of the signal at low pump intensity. For $I < I_{sat}$, the saturation intensity, the measured signal is calculated to be proportional to I^2. However, for $I > I_{sat}$, the signal behavior is strongly dependent on the detector parameters and the input pulse shape. The low-intensity behavior is thus similar to that predicted by the steady-state theory, whereas the saturation behavior will be markedly different.

In the case of long laser pulse, such as that of Fig. 2, with similar detector conditions, the pulsed signal behavior is virtually indistinguishable from that of the steady-state situation of Ref. 5, viz., the signal $I_s \propto I^2$ for $I < I_{sat}$ and $I_s \propto I^{-2}$ for $I > I_{sat}$ (in the Doppler-broadened regime). The experiments to be described in Sec. III involved a laser pulse duration, atomic lifetime, and detector aperture time all of similar values. It is clear from the foregoing theory that care must be exercised in interpreting the signal dependence on pump intensity for pulsed lasers when $I \geq I_{sat}$. However, it is also clear that under suitable conditions, and sufficiently low intensities, the steady-state theory provides an adequate description. This will be the case for the experiment described below to measure the spectral line shape of the DFWM signal generated by broad-bandwidth pumps.

The main theoretical results are illustrated in Fig. 3 where the DFWM reflectivity R is plotted logarithmically against the normalized pump intensity for three values of the laser bandwidth b. The values of b in this figure correspond to the values used in the experimental measurements to be described in the following section. The general behavior of the calculated signals has been discussed fully in Ref. 5. We note here again that good agreement between theory and experiment cannot be expected at intensity levels approaching and exceeding the saturation level. However, up to this level the steady-state results give an adequate description of the signal dependence on pump intensity.

III. EXPERIMENT

The main aim of the experimental work was to measure the DFWM reflectivity as a function of pump intensity and to determine the effect of laser bandwidth on this dependence. Two situations of interest were studied; first when the pump lasers were tuned to, or close to, the atomic resonance $\Delta = 0$; and second for the off-resonance interaction $\Delta \neq 0$. A further aim of the work was to determine the line shape of the DFWM signal induced by broad-bandwidth pumps and a monochromatic probe. Each of the experiments required a pump beam which approximated to a chaotic field and whose bandwidth could be continuously varied. A tunable, "modeless" dye laser developed previously by one of us was used to provide the broad, variable bandwidth radiation.[11]

A. Pump intensity dependence of DFWM reflectivity

A schematic representation of the experimental apparatus is shown in Fig. 4. The nonlinear medium consisted of atomic sodium vapor contained in a simple resistively heated cell. The vapor was confined to a region

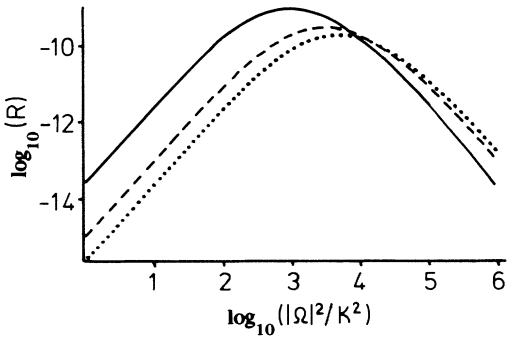

FIG. 3. Logarithmic plot of theoretical DFWM reflectivity R against pump intensity normalized to the saturation intensity. These results have taken into account the Doppler effect. The effect of the laser bandwidth b is shown by the three curves as follows: solid line $b = 1100\kappa$, dashed line $b = 3300\kappa$, dotted line $b = 5300\kappa$.

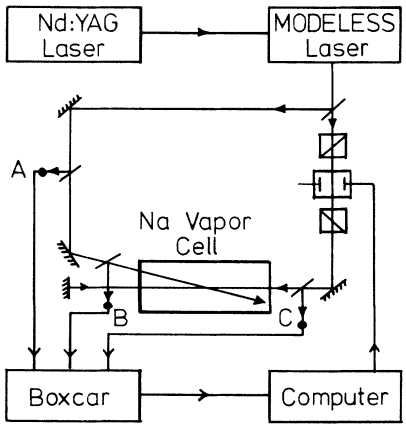

FIG. 4. Schematic representation of the experimental layout used to determine the DFWM reflectivity as a function of laser bandwidth. A, B, and C indicate photodetectors for monitoring the intensity of input laser and reflected signal beams.

5–10 mm in length by a baffle system and the number density was maintained at 10^{10}–10^{11} cm^{-3} with about 10 mbar of argon present as a buffer gas. The sodium density was monitored during the course of the experiments by measuring the attenuation of a weak beam of single mode cw dye laser radiation (linewidth ~2 MHz) tuned to the center of the D_2 resonance line. This monitoring ensured that the experiments were carried out under effectively optically thin conditions. In addition, it allowed changes in the signal strength owing to density variations with time to be normalized. This normalization was necessary to account for a slow drift in the vapor conditions which occurred over the several hours needed to complete a sequence of data acquisition.

The broad-bandwidth laser radiation was obtained from a modeless dye-laser system, details of which are given in Ref. 11. This device and a subsequent amplifier stage was pumped by the frequency doubled output of a Q-switched Nd:YAG laser (YAG denotes yttrium aluminum garnet) to give a pulse energy of approximately 1.0 mJ and of duration ~10 ns. The output of the dye-laser system had a continuous frequency spectrum with a bandwidth variable over the range 15–150 GHz.

The reflected DFWM signal was directed by a beam splitter to a photomultiplier (1P28 type) whose output was sampled by a boxcar averager. The single shot signal level was recorded and stored by a microcomputer. The intensity of the pump beams was monitored by a second photomultiplier and the values similarly sampled and recorded by the same boxcar averager and microcomputer. The intensity of the pump beams was varied on passing through an electro-optic modulator system consisting of a Pockels cell between crossed calcite-prism polarizers. The voltage applied to the device and its resulting transmission was regulated under control of the microcomputer.

A fraction of the laser output was reflected from an uncoated glass beam splitter, spatially filtered and attenuated to provide a low-intensity probe beam about 1 mm in diameter and of approximately Gaussian intensity profile. The remainder of the beam was used to form the counterpropagating pump beams. The optical paths were adjusted to ensure a zero delay between the probe and the forward going pump. This ensured that signal variations were not generated by changes in the coherence length when the bandwidth was varied.[12] The backward going pump beam was delayed by ~500 mm, a distance greater than the coherence lengths for all of the bandwidths used, to ensure that the pump beams could be copolarized but uncorrelated as assumed in the theory.

The expanded pump beams were directed along the axis of the Na vapor cell, where they had a diameter of approximately 10 mm. Crossing the pump beams at an angle of ~3° at the center of the cell, the 1-mm-diameter probe beam then intersected an approximately uniform pump field allowing the experimental results to be compared with the theory which assumed plane waves in the interaction region.

The bandwidth of the beams was measured by a pressure scanned Fabry-Pérot étalon (instrumental width ~1 GHz) for narrow bandwidths in the range 10–30 GHz, and by a monochromator for those in the range 30–150 GHz. The effective resolution limit for the monochromator was ~5 GHz. The detuning of the laser from atomic resonance Δ was also measured using the monochromator by simultaneously scanning across the laser spectrum and that of a hollow cathode Na lamp.

The values of DFWM signal, and hence reflectivity, were recorded as a function of pump intensity by the microcomputer for each value of laser bandwidth. The averaged data was then normalized in proportion to the square of the atomic number density to take account of long-term drifts in the vapor conditions in the cell. The signal was also measured as a function of probe intensity to ensure, by its linear dependence, that the signals were generated in the linear, undepleted pump regime.

B. Results

In Fig. 5 we show the variation of the DFWM signal as a function of pump intensity I for three values of laser bandwidth, with the laser tuned close to atomic resonance $\Delta \simeq 0$. For low intensities the results show that the reflectivity R is proportional to I^2, in agreement with theory. The dependence on bandwidth, for pump and probe bandwidths equal to b, is given by $R \propto b^{-m}$ with $m = 2.1 \pm 0.9$, which is in reasonable agreement with the theoretical value of $m = 3$. The large uncertainty in the experimental value of m arises largely from uncertainty in the normalization factors used to normalize for drift in the atomic number density and the relative intensity calibrations of low-intensity signals.

The absolute value of the saturation intensity is of the order of $1000\kappa^2$, broadly in agreement with the predicted values of $b\kappa$. Theoretically we expect the value of I_{sat} to scale with b^q with $q = 1$, whereas experimentally we find q to be approximately 0.3. The deviation from the expected value may be accounted for by distortions in the curves at high intensities arising from the pulse reshaping effects discussed above. Such effects may be even more

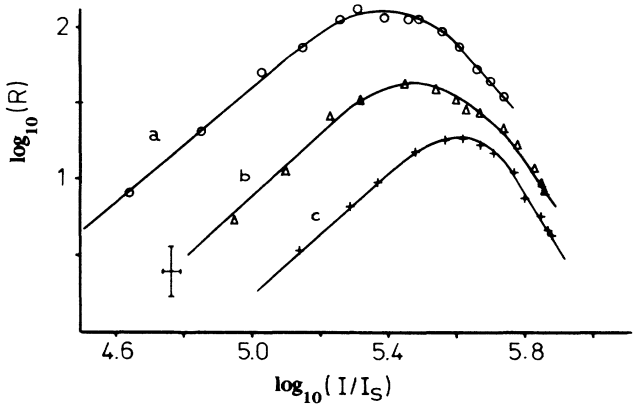

FIG. 5. Logarithmic plot of the experimentally determined DFWM reflectivity R as a function of pump intensity I (in units of I_s) for different laser bandwidths: curve (*a*) $b = 1100/\kappa$, curve (*b*) $b = 3300/\kappa$, curve (*c*) $b = 5300/\kappa$. The error bar indicates the uncertainty in the relative positions of the three curves owing to the uncertainty in the relative atomic vapor density.

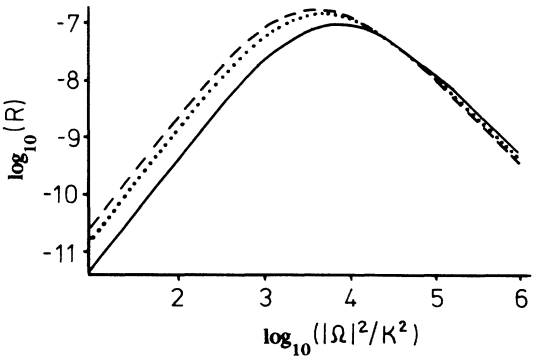

FIG. 6. Logarithmic plot of theoretical reflectivity R as a function of pump intensity normalized to the saturation intensity for a laser detuning of $\Delta = 2000\kappa$. Laser bandwidths are 800κ (solid curve), 3000κ (dashed curve), 4600κ (dotted curve). Note that the bandwidth-dependent saturation intensity (the peak of each curve) first shifts to a lower value as b increases from a value $< \Delta$ and then shifts to a higher value for $b > \Delta$.

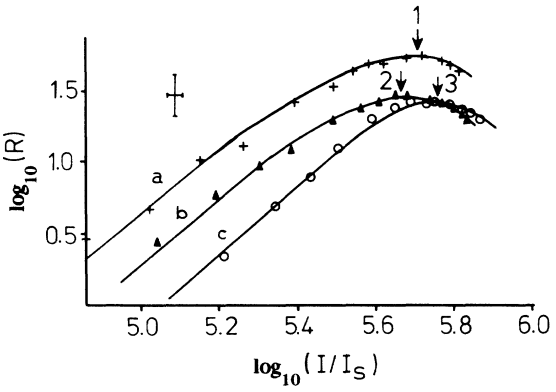

FIG. 7. Logarithmic plot of experimentally determined reflectivity R as a function of pump laser normalized to the saturation intensity for the values of detuning Δ, and bandwidth b shown in the theoretical plot of Fig. 6, viz., $\Delta = 2000\kappa$, curve (a) $b = 800\kappa$; curve (b) $b = 3000\kappa$; curve (c) $b = 4600\kappa$. The error bar shows the uncertainty in the relative positions of the three curves. The peaks of these curves are marked by arrows 1, 2, and 3, respectively, showing the theoretically predicted trend.

important for $I > I_{sat}$, where the experimental curves decrease at a rate faster than the I^{-2} dependence predicted by the theory. At these high intensities additional problems of self-focusing may also contribute to a faster than expected decline in the signal.

For broad-bandwidth lasers detuned from resonance ($\Delta > 0$) we expect a somewhat different dependence of the saturation intensity I_{sat} on the laser bandwidth b. Figure 6 shows the calculated signal dependence on I for three values of b increasing from $b < \Delta$ to $b > \Delta$. As b increases from a value less than Δ, there is an increasingly effective overlap with the atomic resonance, leading to a reduction in the value of I_{sat}. However, when $b > \Delta$ a further increase in bandwidth results in a less effective resonance interaction and I_{sat} increases as observed in the previous case of $\Delta = 0$. So, for broadband lasers detuned by an amount Δ, greater than the initial bandwidth b, we expect the saturation intensity I_{sat} to first decrease as b increases, then to increase as the bandwidth becomes larger than the detuning.

In Fig. 7 we show the results of measurements taken with a fixed value of $\Delta = 50$ GHz. For the three values of b used, 15, 60, and 93 GHz, we note the initial reduction in I_{sat} as b is increased from its narrowest value, followed by an increase in I_{sat} when $b > \Delta$. These results show the expected trend and are thus in qualitative agreement with the theory. It will be noticed that the curve showing the experimentally determined reflectivity R in the case of the narrowest bandwidth used (15 GHz or $\sim 800\kappa$) lies higher than those for the larger bandwidths, whereas the theory would predict it to lie lower. We have no quantitative explanation for this effect, but several of the factors mentioned above would tend to give this inversion. Notably, the uncertainty in the relative number density of sodium atoms during the taking of the three sets of data leads to a corresponding uncertainty in the relative positions of the curves for bandwidths which differ by less than an order of magnitude. Also, a small amount of absorption, at line center, of the beams as they propagate to the interaction region will reduce the effectiveness of the DFWM process. This will affect the narrow-bandwidth beams to a lesser extent than the broader-bandwidth beams, thus giving a relative enhancement in the narrow-bandwidth case.

C. FWM line shapes with broad-bandwidth pumps

If pump and probe fields are degenerate in frequency and of an equal bandwidth b, which is much less than the Doppler width, it has been shown that the spectral response of the DFWM signal as a function of Δ is "Doppler-free." This feature has made narrow-bandwidth DFWM useful as a high-resolution spectroscopic tool.[13] Doppler-free spectra may be generated with narrow linewidth pulsed lasers as shown in Fig. 8(a). This spectrum was obtained by recording the DFWM signal as the frequency of a pulse amplified single-mode cw dye laser was scanned through the D_2 resonance line of atomic Na. The cw dye-laser beam was amplified on passing through two dye cells, transversely pumped by a frequency doubled dye laser. The resulting pulses had a measured linewidth of $\Delta\omega_L \sim 300$ MHz. The linewidth of the spectra is thus limited to this laser linewidth $\Delta\omega_L$. However, since $\Delta\omega_L < \Delta\omega_D$, the Doppler width, the hyperfine structure can still be clearly resolved although there is some degree of power broadening. In the opposite limit, where $\Delta\omega_L > \Delta\omega_D$, then again the linewidth of the spectra would be determined by the laser linewidth, and no information on the atomic frequency response would be obtained.

We have carried out an experiment on an intermediate case where the pump laser linewidth $b > \Delta\omega_D$, but the probe laser is essentially monochromatic, $p \ll \Delta\omega_D$. In this experiment the frequency of the broadband pumps was fixed at line center $\Delta = 0$. The signal was then recorded as a function of the detuning Δ_2 between probe

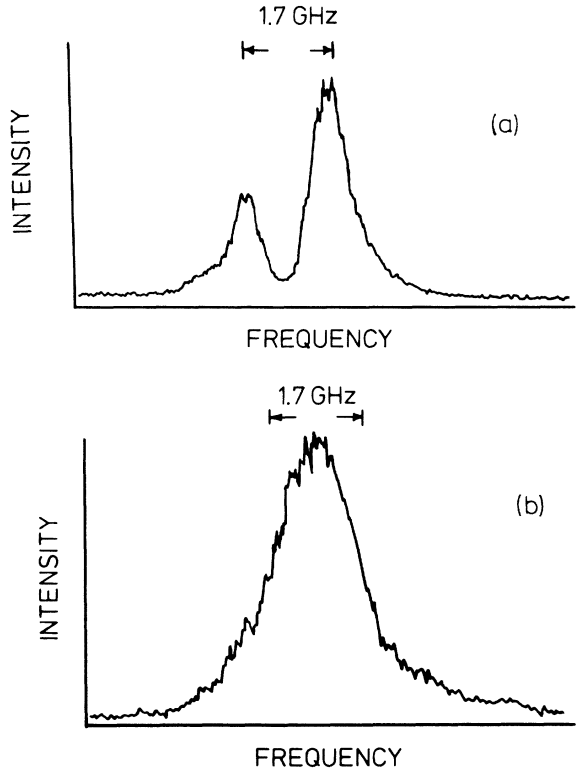

FIG. 8. (a) DFWM spectrum obtained by scanning the frequency of both pump and probe beams, derived from a pulse-amplified single-mode laser (linewidth ~300 MHz), across the D_2 line of atomic Na showing power-broadened hyperfine structure lines. (b) DFWM spectrum obtained by scanning the frequency of a narrow-bandwidth probe beam (linewidth ~300 MHz) across the same D_2 line with broadband pump beams (linewidth ~20 GHz) fixed on resonance ($\Delta=0$). The profile is now a Gaussian, Doppler-broadened line shape as predicted by the theory.

beam and pumps. The broadband pumps were provided by the modeless laser as before, and were arranged to have a linewidth $b \sim 20$ GHz. The narrow-band probe was provided by a pulse-amplified single-mode cw dye laser (Coherent 599-21) with a linewidth of $\Delta\omega_L \sim 300$ MHz. The spectrum obtained on tuning the probe through resonance is shown in Fig. 8(b). It is evident that the linewidth is determined here by the Doppler width with an approximately Gaussian profile.

We have shown in our previous work that for a probe of bandwidth p, interacting with pumps of broad bandwidth b, the FWM reflectivity as a function of the probe's detuning from atomic resonance Δ_2 is given by

$$R(\Delta_2)=\frac{\kappa\varphi^2}{16\Delta\omega_D(1+2\varphi)^3}\frac{1}{d^2(\alpha+d)} \times\left[\frac{(\alpha-d)}{1+[2\alpha^2/\kappa(1+2\varphi)]}\right] \times\int\frac{\gamma_0 W(v)dv}{(\Delta_2-k_3v)^2+\gamma_0^2},$$

with $\gamma_0=2\Gamma+\kappa(1+\varphi)+p$,

$$\varphi=\frac{|\Omega|^2}{\kappa}\frac{b}{b^2+\Delta^2},$$

$$\alpha=(\Gamma+\kappa\varphi)^{1/2},$$

$$d=\left[\alpha^2-\frac{\kappa\varphi^2}{1+2\varphi}\right]^{1/2},$$

$$W(v)=\left[\frac{m}{2\pi kT}\right]^{1/2}\exp-(kv/\Delta\omega_D)^2.$$

$\Delta\omega_D$ is the Doppler width and $\Delta \ll b$. The response is a convolution of the Doppler and laser spectral profiles. For small values of the pump bandwidth $b<\Delta\omega_D$, the response is Doppler-free. Conversely, for $b>\Delta\omega_D$, the line shape is determined by the Doppler profile as verified in the result shown in Fig. 8(b).

IV. CONCLUSION

We have presented here the results of an attempt to quantify the effects of laser bandwidth on the process of DFWM. We have developed a time-dependent theory of FWM that is valid for arbitrary pulse shapes and intensities in the cases where the laser bandwidth exceeds all other relaxation rates in the problem. In a series of experiments we have measured the effect of laser bandwidth on the pump intensity dependence of DFWM signals. Qualitative agreement between experiment and theory has been observed. Quantitative agreement was not as good, especially in those features involving intensities which approached or exceeded the bandwidth-dependent saturation level. Several factors may be cited to account for the disparity—especially at the high-intensity ranges.

First, the theory assumes a Lorentzian line shape which is not generally realized in the output of most lasers—or the one employed in this study. Second, all propagation effects are ignored in the theory. In practice, a certain amount of absorption will occur, especially at line center, resulting in a change in the effective laser intensity in the interaction region. A further effect of such absorption will be a distortion of the spectral line shape of the incident fields. A third and very important factor is the pulse reshaping that occurs at high intensities as a result of saturation effects. This process may seriously modify the measured responses at high intensities. Furthermore, uncertainties owing to drifts in vapor conditions in the experiment lead to errors of scaling the relative signal levels measured at different bandwidths. Some attempt to moderate these effect was made by monitoring the total optical thickness of the cell—but a degree of uncertainty remains. Finally, it is possible that nonuniformities in the pump beams could lead to spatially-dependent saturation behavior that could not be accurately monitored.

Given the limitations of the theoretical model and the experimental uncertainties, the results do show reasonable agreement and so do give plausible verification of the

theory. Good agreement was obtained between theory and experiment in measurements of the spectral line shape of the FWM signal produced with broad-bandwidth pumps and a monochromatic probe. As expected, this was found to be Doppler limited in contrast to the case of broad-bandwidth pump and probe or the case of all monochromatic beams where the line shapes are limited by the laser bandwidth or the Doppler-free homogeneous width, respectively.

ACKNOWLEDGMENTS

This work was supported by a grant from the Science and Engineering Research Council (United Kingdom) and two of us (D.R.M.) and (A.C.) are grateful to the Council for personal financial support. J.C. was supported in part by National Science Foundation Grants No. PHY86-04504 and No. INT86-02095 and the William Evans Fund while on leave at the University of Otago, New Zealand.

---

*Present address: Schuster Laboratory, University of Manchester, United Kingdom.

[1]H. J. Kimble and L. Mandel, Phys. Rev. A **15**, 689 (1977); L. A. Lompre, G. Mainfray, C. Manus, and J. P. Mannier, J. Phys. B **14**, 4307 (1981); D. E. Nitz, A. V. Smith, M. D. Levenson, and S. J. Smith, Phys. Rev. A **24**, 288 (1981); P. B. Hogan, S. J. Smith, A. T. Georges, and P. Lambropoulos, Phys. Rev. Lett. **41**, 229 (1978).

[2]S. Asaka, H. Nakatsuka, M. Fujiwara, and M. Matsuoka, Phys. Rev. A **29**, 2286 (1984); N. Morita and T. Yajima, *ibid.* **30**, 2525 (1984); J. E. Golub and T. W. Mossberg, J. Opt. Soc. Am. B **3**, 554 (1986).

[3]L. A. Rahn, R. L. Farrow, and R. P. Lucht, Opt. Lett. **9**, 223 (1984); R. J. Hall and D. A. Greenhalgh, J. Opt. Soc. Am. B **3**, 1637 (1986); P. Narum, M. D. Skeldon, and R. W. Boyd, IEEE J. Quantum Electron. **QE-22**, 2161 (1986); S. Kroll, M. Alden, T. Berglind, and R. J. Hall, Appl. Opt. **26**, 1068 (1987).

[4]*Optical Phase Conjugation*, edited by R. A. Fisher (Academic, New York, 1983).

[5]J. Cooper, A. Charlton, D. R. Meacher, P. Ewart, and G. Alber, Phys. Rev. A **40**, 5705 (1989).

[6]R. L. Abrams and R. C. Lind, Opt. Lett. **2**, 94 (1978); **3**, 205 (1978).

[7]D. S. Elliot, M. W. Hamilton, K. Arnett, and S. J. Smith, Phys. Rev. Lett. **53**, 439 (1984).

[8]M. S. Barashkov and N. A. Iskanderov, Sov. J. Quantum Electron. **17**, 1077 (1987).

[9]A. T. Georges, Phys. Rev. A **21**, 2034 (1980).

[10]M. Kaczmarek, D. R. Meacher, and P. Ewart, J. Mod. Opt. (to be published).

[11]P. Ewart, Opt. Commun. **55**, 124 (1985).

[12]W. M. Grossman and D. M. Shemwell, J. Appl. Phys. **51**, 914 (1980).

[13]R. L. Abrams, J. F. Lam, R. C. Lind, D. G. Steel, and P. F. Liao, in *Optical Phase Conjugation* (Ref. 4), p. 211.